

Influence of basal melanin in the electromagnetic response of regular and weakly disordered photonic crystals

Influencia de la melanina basal en la respuesta electromagnética de cristales fotónicos regulares y débilmente desordenados

G. Urquía¹, M. Lester², M. Inchaussandague^{1,3}, and D. Skigin^{1,3,*}

1. *Universidad de Buenos Aires, Facultad de Ciencias Exactas y Naturales, Departamento de Física, Grupo de Electromagnetismo Aplicado, Buenos Aires, Argentina*
2. *IFAS (UNCPBA) and CIFICEN (UNCPBA-CICPBA-CONICET), Grupo Óptica de Sólidos-Elfo, 7000 Tandil, Buenos Aires, Argentina.*
3. *CONICET - Universidad de Buenos Aires, Instituto de Física de Buenos Aires (IFIBA), Buenos Aires, Argentina*

(*) E-mail: dcs@df.uba.ar

Received: 26/06/2023 Accepted: 02/07/2023
DOI: 10.7149/OPA.56.2.51156

ABSTRACT:

Motivated by the structural color generation in the plumage of some species of birds, which in their barbs combine a quasi-regular arrangement of air voids in a keratin matrix (spongy matrix) backed by melanin granules, in this work we study the influence of basal melanin on the optical response of regular and weakly disordered photonic crystals. By applying two rigorous electromagnetic methods, we investigate the effect produced by a basal layer of melanin granules on the reflected response of regular and slightly irregular photonic crystals comprising infinite cylinders (2D) or spheres (3D). The results show that even for a few layers of scatterers, the reflected response is governed by the geometry, distribution and materials comprising the spongy matrix, and is only weakly dependent on the presence of melanin. This result is found for both 2D and 3D structures, and for finite and infinite systems, indicating a general trend.

Key words: color, photonic crystals, melanin

RESUMEN:

Motivados por la generación de color estructural en el plumaje de algunas especies de aves, que en sus barbas combinan una disposición cuasi regular de huecos de aire en una matriz de queratina (matriz esponjosa) con una capa de gránulos de melanina en su base, en este trabajo estudiamos la influencia de la base de melanina en la respuesta óptica de cristales fotónicos regulares y débilmente desordenados. Mediante la aplicación de dos métodos electromagnéticos rigurosos, investigamos el efecto producido por una capa basal de gránulos de melanina sobre la respuesta reflejada de cristales fotónicos regulares y ligeramente irregulares que comprenden infinitos cilindros (2D) o esferas (3D). Los resultados muestran que incluso para unas pocas capas de dispersores, la respuesta reflejada se rige por la geometría, la distribución y los materiales que componen la matriz esponjosa, y solo depende débilmente de la presencia de melanina. Este resultado se verifica tanto para estructuras 2D como 3D, y para sistemas finitos e infinitos, indicando una tendencia general.

Palabras clave: color, cristales fotónicos, melanina

REFERENCES AND LINKS / REFERENCIAS Y ENLACES

- [1] R. Prum, R. Torres, S. Williamson, and J. Dyck, "Two-dimensional fourier analysis of the spongy medullary keratin of structurally coloured feather barbs," *Proc. Royal Soc. Lond. B* **266**, 13–22 (1999).



- [2] V. Saranathan, J. Forster, H. Noh, S. Liew, S. Mochrie, H. Cao, E. Dufresne, and R. Prum, "Structure and optical function of amorphous photonic nanostructures from avian feather barbs: a comparative small angle x-ray scattering (SAXS) analysis of 230 bird species," *J. Royal Soc. Interface* **9**, 2563–2580 (2012).
- [3] H. Noh, S. F. Liew, V. Saranathan, S. G. J. Mochrie, R. O. Prum, E. R. Dufresne, and H. Cao, "How noniridescent colors are generated by quasi-ordered structures of birds feathers," *Adv. Mater.* **22**, 2871–2880 (2010).
- [4] C. D'Ambrosio, M. Inchaussandague, D. Skigin, A. Barreira, and P. Tubaro, "Structural colour in *Tersina viridis*," *Opt. Pura y Apl.* **50**, 279–288 (2018).
- [5] C. D'Ambrosio, D. Skigin, M. Inchaussandague, A. Barreira, and P. Tubaro, "Structural color in the swallow tanager (*Tersina viridis*): Using the Korringa-Kohn-Rostoker method to simulate disorder in natural photonic crystals," *Phys. Rev. E* **98**, 032403 (2018).
- [6] D.-J. Jeon, S. Ji, E. Lee, J. Kang, L. D'Alba, M. D. Shawkey, and J.-S. Yeo, "How the Eurasian jay expands its color palette by optimizing multiple scattering," *Adv. Opt. Mater.* **11**, 2202210 (2023).
- [7] M. D. Shawkey and G. E. Hill, "Significance of a basal melanin layer to production of non-iridescent structural plumage color: evidence from an amelanotic steller's jay (*Cyanocitta stelleri*)," *J. Exp. Biol.* **209**, 1245–1250 (2006).
- [8] Y. Zhang, B. Dong, L. Shi, H. Yin, X. Liu, and J. Zi, "Color production in blue and green feather barbs of the rosy-faced lovebird," *Mater. Today: Proc.* **15**, 130 – 137 (2014).
- [9] M. D. Shawkey, S. L. Balenger, G. E. Hill, L. S. Johnson, A. J. Keyser, and L. Siefferman, "Mechanisms of evolutionary change in structural plumage coloration among bluebirds (*Sialia spp.*)," *J. Royal Soc. Interface* **3**, 527–532 (2006).
- [10] M. Fan, L. D'Alba, M. D. Shawkey, A. Peters, and K. Delhey, "Multiple components of feather microstructure contribute to structural plumage colour diversity in fairy-wrens," *Biol. J. Linnean Soc.* **128**, 550–568 (2019).
- [11] A. Barreira, "Evolución de los patrones de coloración del plumaje en fruteros neotropicales," Ph.D. thesis, University of Buenos Aires, Argentina (2011).
- [12] G. M. Urquia, M. E. Inchaussandague, D. C. Skigin, M. Lester, A. Barreira, and P. Tubaro, "Theoretical approaches to study the optical response of the red-legged honeycreeper's plumage (*Cyanerpes cyaneus*)," *Appl. Opt.* **59**, 3901–3909 (2020).
- [13] M. Xiao, Y. Li, M. C. Allen, D. D. Deheyn, X. Yue, J. Zhao, N. C. Gianneschi, M. D. Shawkey, and A. Dhinojwala, "Bio-inspired structural colors produced via self-assembly of synthetic melanin nanoparticles," *ACS Nano* **9**, 5454–5460 (2015).
- [14] M. Xiao, Z. Hu, Z. Wang, Y. Li, A. D. Tormo, N. L. Thomas, B. Wang, N. C. Gianneschi, M. D. Shawkey, and A. Dhinojwala, "Bioinspired bright noniridescent photonic melanin supraballs," *Sci. Adv.* **3**, e1701151 (2017).
- [15] M. Iwata, M. Teshima, T. Seki, S. Yoshioka, and Y. Takeoka, "Bio-inspired bright structurally colored colloidal amorphous array enhanced by controlling thickness and black background," *Adv. Mater.* **29**, 1605050 (2017).
- [16] P. Shi, E. Miwa, J. He, M. Sakai, T. Seki, and Y. Takeoka, "Bioinspired color elastomers combining structural, dye, and background colors," *ACS Appl. Mater. Interfaces* **13**, 55591–55599 (2021).
- [17] A. Maradudin, T. Michel, A. R. McGurn, and E. R. Méndez, "Enhanced backscattering of light from a random grating," *Annals Phys.* **203**, 255–307 (1990).
- [18] R. Carminati, A. Madrazo, and M. Nieto-Vesperinas, "Electromagnetic wave scattering from a cylinder in front of a conducting surface-relief grating," *Opt. Commun.* **111**, 26–33 (1994).
- [19] M. Lester and D. Skigin, "Coupling of evanescent s-polarized waves to the far field by waveguide modes in metallic arrays," *J. Opt. A: Pure Appl. Opt.* **9**, 81–87 (2007).
- [20] O. V. Belai, L. L. Frumin, S. V. Perminov, and D. A. Shapiro, "Scattering of evanescent electromagnetic waves by a cylinder near the flat boundary: the green function and fast numerical method," *Opt. Lett.* **36**, 954–956 (2011).
- [21] R. M. A. Ekeroth and M. F. Lester, "Optical forces on silver homogeneous nanotubes: Study of shell plasmonic interaction," *Plasmonics* **10**, 989–998 (2015).
- [22] N. Stefanou, V. Yannopoulos, and A. Modinos, "Heterostructures of photonic crystals: frequency bands and transmission coefficients," *Comput. Phys. Commun.* **113**, 49–77 (1998).



- [23] N. Stefanou, V. Yannopapas, and A. Modinos, "Multem 2: a new version of the program for transmission and band structure calculations of photonic crystals," *Comput. Phys. Commun.* **132**, 189–196 (2000).
- [24] H. L. Leertouwer, B. D. Wilts, and D. G. Stavenga, "Refractive index and dispersion of butterfly scale chitin and bird feather keratin measured by interference microscopy," *Opt. Express* **19**, 24061–24066 (2011).
- [25] D. G. Stavenga, H. L. Leertouwer, D. C. Osorio, and B. D. Wilts, "High refractive index of melanin in shiny occipital feathers of a bird of paradise," *Light. Sci. & Appl.* **4**, e243 (2015).
- [26] M. Lester and M. Nieto-Vesperinas, "Optical forces on microparticles in an evanescent laser field," *Opt. Express* **21**, 936–938 (1999).
- [27] L. B. Scaffardi, M. Lester, D. Skigin, and J. O. Tocho, "Optical extinction spectroscopy used to characterize metallic nanowires," *Nanotechnology* **18**, 315402 (2007).
- [28] A. Modinos, "Scattering of electromagnetic waves by a plane of spheres-formalism," *Phys. A* **141**, 575–588 (1987).
- [29] V. Yannopapas, A. Modinos, and N. Stefanou, "Optical properties of metallodielectric photonic crystals," *Phys. Rev. B* **60**, 53–59 (1999).
- [30] V. E. Johansen, O. D. Onelli, L. M. Steiner, and S. Vignolini, *Photonics in Nature: From Order to Disorder* (Springer International Publishing, Cham, 2017), pp. 53–89.
- [31] A. Ishimaru, *Wave Propagation and Scattering in Random Media*, vol. 1 Academic Press, NY, (1970).
- [32] C. Jin, X. Meng, B. Cheng, Z. Li, and D. Zhang, "Photonic gap in amorphous photonic materials," *Phys. Rev. E* **63**, 195107 (2001).
- [33] L. S. Froufe-Perez, M. Engel, P. F. Damasceno, N. Muller, J. Haberko, S. C. Glotzer, and F. Scheffold, "The role of short-range order and hyperuniformity in the formation of band gaps in disordered photonic materials," *Phys. Rev. Lett.* **117**, 053902 (2016).

1. Introduction

In some species of birds, the color appearance is produced by a three-dimensional quasi-ordered nanostructure formed by keratin and air, which is found in their feather barbs and is usually called spongy matrix (SM) [1–6]. The SM can be either of channel type –a disordered channel-like network of spongy β -keratin bars– or sphere type, which comprises a quasi-regular arrangement of spheroidal air cavities immersed in keratin [2]. The feather barbs' microstructure of certain species also include melanin granules. This is the case of the Steller's jay [7], the rosy-faced lovebird [8], the Eurasian jay [6], and several species of the Turdidae [9], the Maluridae [10] and the Thraupidae families [11, 12], to name a few examples. In many cases, these melanin granules appear as a substrate for the SM, although their specific role in the color generation remains only partly understood [6, 7, 9, 10].

Inspired by the large variety of biological examples of microstructures comprising melanin, attention has been recently paid to the use of synthetic melanin in artificial structures, as a means to improve the color saturation and enlarge the color palette. For instance, synthetic melanin nanoparticles were fabricated to generate structural colors [13], to which silica shells were later added in order to tune the brightness and hue of the resulting colors [14]. Also, the importance of the background material and color has been recently assessed by several authors in order to enhance the structural color properties of colloidal arrays of spherical nanoparticles [15, 16]

The objective of this work is to study the influence of basal melanin on the optical response of perfectly regular and weakly disordered photonic crystals, in order to contribute to the design of the color appearance of bioinspired artificial materials. In particular, we focus on the response of nanostructures with inclusions of sizes and separations typically found in avian feather barbs. To calculate the optical response of the structures we use the integral method (IM), a rigorous method based on the second Green's identity [17]. The IM was widely used to deal with a large variety of 2D scatterers [18–21] and has the advantage of being very versatile regarding the geometry and distribution of the scattering objects and the constitutive parameters of the materials involved. In particular, it has been recently applied to model the reflectance spectra of avian feathers [12]. In order to extend our study and investigate the role of basal melanin not only for 2D photonic crystals but also for 3D structures, we employ the Korringa-Kohn-Rostoker formalism (KKR), which allows calculating the reflectance of finite systems that may



combine layers of periodically arranged spheres with layers of homogeneous materials [22, 23]. By comparing the results obtained by both methods, we are able to arrive to a more general conclusion about the importance of basal melanin in the reflectance response.

In Section 2, we describe the analyzed structures and briefly explain the electromagnetic methods employed to compute the reflected response. The results obtained are shown in Section 3, where we present calculated reflectance spectra for structures comprising regular and weakly irregular distributions of scatterers, with and without basal melanin. To complete the study, we also show near field distributions at particular wavelengths. Finally, a discussion and concluding remarks are given in Section 4.

2. Electromagnetic Modelling

Taking into account the motivation of this study, the materials involved in the investigated structures are keratin, melanin and air. For the refractive index of keratin, we used $n_k = 1.58$ [2, 5]. The absorption and dispersion by melanin is taken into account through its complex refractive index $n_m = \eta_m + i\kappa_m$. For its real part we used the Cauchy formula $\eta_m = A + B/\lambda^2$, with $A = 1.648$ and $B = 23700 \text{ nm}^2$, and for the imaginary part we considered $\kappa_m = Ce^{-\lambda/D}$, with $C = 0.56$ and $D = 270 \text{ nm}$ [24, 25].

2.a. Analysis of Structures Formed by Cylinders: Integral Method

The IM is a very versatile rigorous approach to simulate scattering processes from objects of complex shapes [17]. It is particularly suitable to compute the electromagnetic response of systems comprising bodies of arbitrary geometry, distribution and constitutive parameters of the materials involved. In this work we employ a generalization of the method presented in [17] for systems with translation symmetry, usually called 2D problems [18], in which the scattering objects are infinite cylinders. Apart from some depolarization effects, this calculation reproduces the same phenomena as the full 3D calculation; hence, it allows an understanding of the basic physical processes involved in the near-field optical interaction, with a lower computational cost and without loss of generality [20, 21, 26, 27]. For the 2D case, the general scattering problem can be separated into two polarization modes: S polarization (electric field parallel to the cylinders' axes) and P polarization (magnetic field parallel to the cylinders' axes).

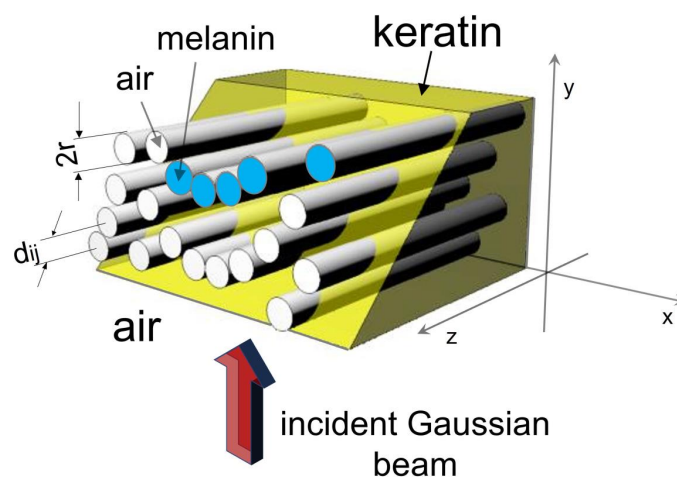


Fig. 1. Scheme of the 2D cylinders' structure investigated with the IM. A finite number of air and melanin cylinders, all of radius r , located at arbitrary positions and immersed in keratin are illuminated by a Gaussian beam. d_{ij} represents the distance between the i -th and j -th cylinder.

Therefore, the vectorial problem is reduced to two scalar problems [19]. Using Green's second integral theorem and the extinction theorem for multiply connected scattering domains [17, 18], we obtain exact expressions for the scattered electromagnetic field produced by a S- or a P-polarized beam of finite width, incident onto an inhomogeneous dielectric medium that contains the scatterers. As a result, the problem is reduced to the solution of a $2N \times 2N$ system of coupled equations (N is the number of spatial points employed to sample the scattering objects), whose unknowns are the electric and the magnetic fields and their normal derivatives at each of the scatterers' boundaries. In this way, it is possible to reconstruct the electromagnetic fields in every point of space and, in particular, the intensity of the reflected and transmitted far field, from which the reflectance and the transmittance can be obtained.

The modelled scattering system comprises a finite set of parallel infinitely long cylinders immersed in an isotropic, linear and homogeneous dielectric medium (see Fig. 1). Therefore, the spatial domains are delimited by circles (cylinders' cross section) at each interface that separates the cylinder from the host medium. The structure is normally illuminated from air ($y < 0$) by a finite linearly polarized Gaussian beam of wavelength λ and half-width $W = 5 \mu\text{m}$, as shown in Fig. 1. For a structure of finite size, the total reflectance includes the contributions of the light scattered in all directions.

2.b. Analysis of Structures Formed by Spheres: KKR Method

Among the methods available for the calculation of the electromagnetic response of composite periodic structures made of spheres, the KKR appears to be numerically efficient. Within its framework, the electromagnetic interactions between the inclusions arranged in the periodic lattice are calculated by means of the layer-multiple scattering method for spherical scatterers [22, 23, 28, 29]. The crystal can be considered as a stack of parallel layers of spheres periodically arranged in a 2D Bravais lattice.

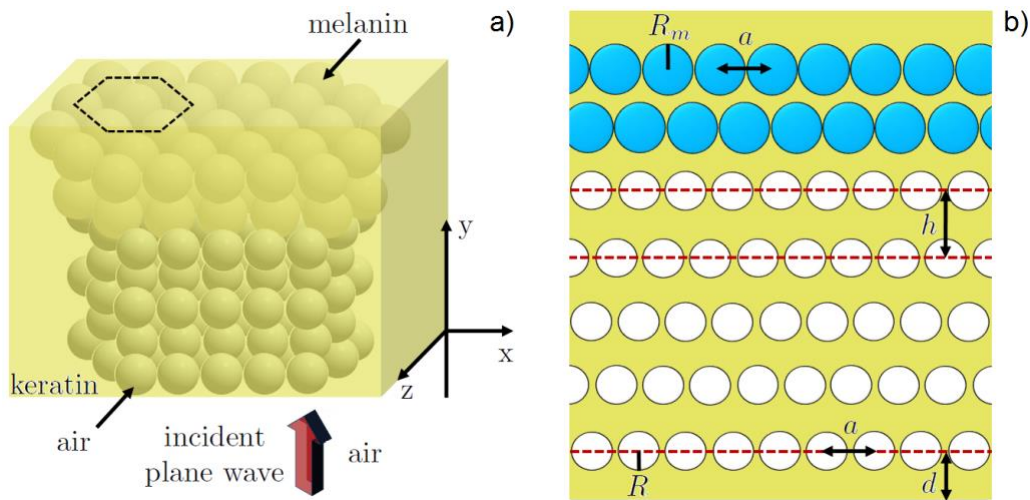


Fig. 2. (a) Scheme of the 3D spheres' structure investigated with the KKR. A hexagonal arrangement of air spheres immersed in keratin is illuminated by a linearly polarized plane wave. In the scheme, two layers of melanin spheres are shown at the top of the air spheres. (b) A cross-section view of the structure at the x - y plane. The geometrical parameters are indicated.

To solve the electromagnetic problem, the multiple scattering between spheres of each single layer is calculated first. Then, the scattered response of multiple layers is determined by using a procedure similar to the one used to calculate the reflection and transmission properties of stratified media with planar interfaces. The computer program MULTTEM [22, 23] is the numerical implementation of the KKR employed in this work.

We consider a hexagonal array composed of M identical parallel layers of spherical air cavities (radius R) immersed in a keratin matrix (Fig. 2). The lattice constant is a , the parallel layers are separated a distance $h = (\sqrt{3}/2) a$, and the distance from the centers of the air spheres of the bottom layer to the interface is $d = 0.5 a$. To analyze the effect of basal melanin on the optical response, we compare the

results of this structure with those of the same structure but with two additional layers of melanin spheres of radius R_m . These spheres are periodically distributed within the keratin medium and also located at the sites of a hexagonal Bravais lattice with the same lattice constant and the same distance between layers as for the air voids arrangement. All the spheres' structures considered are illuminated by a linearly polarized normally plane wave from air.

3. Results

3.a. Structures Formed by Cylinders

Fig. 3 shows the reflectance curves obtained with the IM for a structure comprising 5 layers of air cylinders and also for the same structure with additional two layers of melanin cylinders, located forming a hexagonal array. We consider air cylinders of radius $r = 82.7$ nm, melanin cylinders of radius $R_m = 110$ nm, and the distance between centers of adjacent cylinders within the same layer is $d = 225$ nm, which are typical values found in the spongy matrix of avian barb [12]. In each panel we show the results for the cases with (hole circles) and without (solid black dots) basal melanin. Panel (a) corresponds to S polarization and (b) to P polarization.

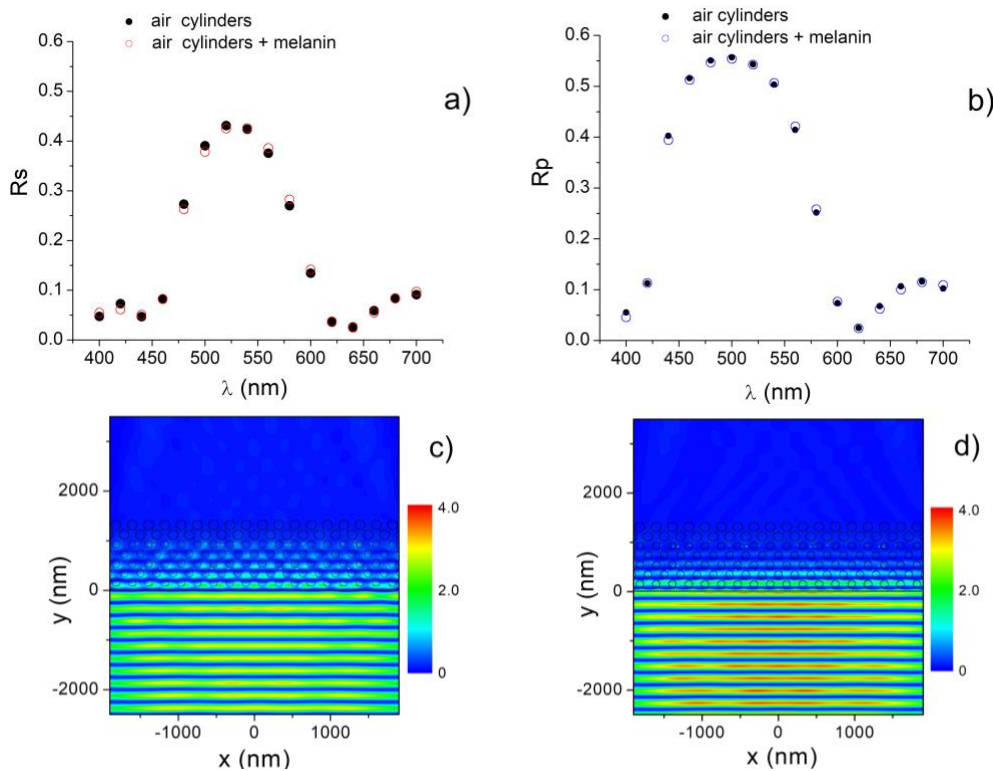


Fig. 3. Reflectance of a regular hexagonal system of 5 layers of air cylinders immersed in keratin, with (hole circles) and without (solid black dots) basal melanin, for S (a) and P (b) polarization. (c)-(d) NF for the hexagonal structure with basal melanin at $\lambda = 500$ nm: (c) S-polarization and (d) P-polarization. Red (blue) indicates highest (lowest) field intensity. The cross-section of the analyzed structure (hexagonal arrangement) is shown as black hole circles within the near field plots.

It is observed that the curves corresponding to both systems, i.e., with and without basal melanin, are almost identical throughout the entire wavelength range investigated. For both structures, an intensification of the reflectance is observed between 450 and 600 nm, associated with a photonic band gap, within which the reflectance reaches a maximum of $\approx 45\%$ for S polarization and almost 60% for P polarization. Clearly, the presence of basal melanin in a perfectly regular structure of cylinders does not alter the reflected response. This behavior is consistent with the near field intensity distribution (NF), defined as $|E|^2/|E_0|^2$ for S polarization and $|H|^2/|H_0|^2$ for P polarization (E_0 and H_0 are the amplitudes of

the incident electric and magnetic field, respectively). In Figures 3(c) and (d) we show NF at $\lambda = 500$ nm for S and P polarization, respectively. It can be noticed that the electromagnetic field penetrates only a few layers within the structure and hardly reaches the melanin layers, producing negligible effect in the reflected response. Similar behavior of the near field is found for other wavelengths outside the band gap (not shown).

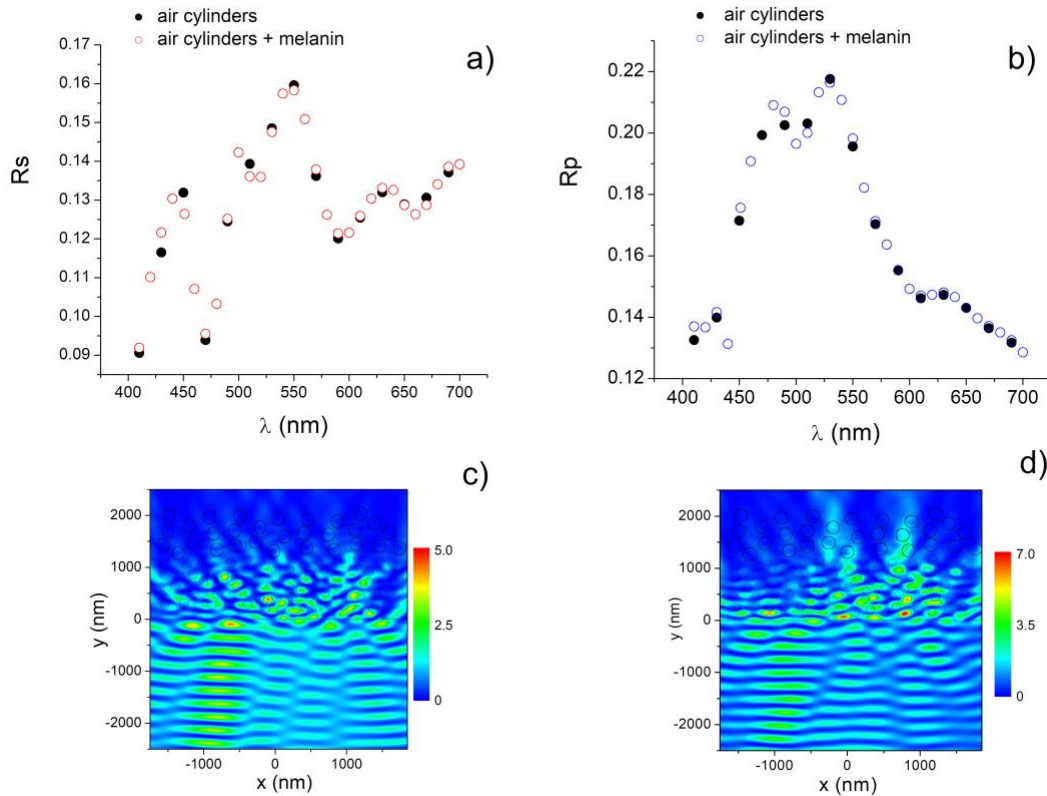


Fig. 4. Reflectance of a weakly disordered arrangement of cylinders immersed in keratin, with (hole circles) and without (solid black dots) basal melanin, for S (a) and P (b) polarization. (c)-(d) NF for the structure with basal melanin at $\lambda = 500$ nm. (c) S-polarization and (d) P-polarization. Red (blue) indicates highest (lowest) field intensity. The cross-section of the analyzed structure is shown as black hole circles within the near field plots.

To investigate whether this behavior is related to the type of arrangement of cylinders, i.e., to the fact that the structure is perfectly regular, in Fig. 4 we show results for a system comprising a weakly disordered distribution of cylinders, and compare the reflectance obtained in the cases with and without basal melanin, for both polarization modes. The cylinders' radii are the same as in Fig. 3, and the positions of the cylinders' centers have been generated starting from the ordered system and adding a perturbation using a random distribution function. The cylinders' distributions considered in this case are shown as black hole circles within the near-field maps (Fig. 4(c)-(d)).

The reflectance curves for the weakly disordered structure differ from those of the regular structure. The reflectance varies approximately between 10 and 15% for S polarization and between 10 and 22% for P polarization. It is interesting to note that even though the structure is no longer regular, the reflectance exhibits maxima of bandwidths comparable to the photonic band gap of the perfectly regular structure (Fig. 3). By comparing the results for the case with (hole circles) and without (solid black dots) basal melanin for each polarization mode, it can be noticed that the addition of basal melanin does not modify significantly the reflected response, as already shown in Fig. 3 for the hexagonal arrays of cylinders. This indicates that the optical response is governed by the spongy matrix, mainly by its distribution and typical size of the scatterers, and it is not very sensitive to the presence of basal melanin. To better understand this result, Figs. 4(c)-(d) show the near field distribution for the cylinders' structure with basal melanin for $\lambda = 500$ nm, for S and P polarization, respectively. Noticeably, the near field patterns in the case of weakly disordered systems of cylinders is more complex than that of the regular system. In this case, the

electromagnetic field penetrates slightly more deeply within the structure, although it seems to be insufficient to produce a significant change in the reflected response. Therefore, we conclude that the presence of basal melanin in weakly disordered arrangements of cylinders does not alter significantly the near field distribution, which, in turn, produces very similar far field responses.

This characteristic is also revealed by the total near field evaluated at a fixed distance from the structure, as shown in Fig. 5. In this Figure we show the near field intensity distribution (NF) at $\lambda = 650$ nm for the systems with and without basal melanin considered in Fig. 4, evaluated at two different y -levels: $y = 2200$ nm (transmitted field) and $y = -1000$ nm (incident and reflected field), for S and P polarizations. It can be noticed that the presence of basal melanin hardly influences the reflected response of the structure (Figs. 5(b) and 5(d)). However, in the transmission region of space (Figs. 5(a) and 5(c)) the differences become more appreciable. Moreover, the integral over all the x -range considered is smaller for the structure containing melanin, indicating that absorption by melanin plays a role.

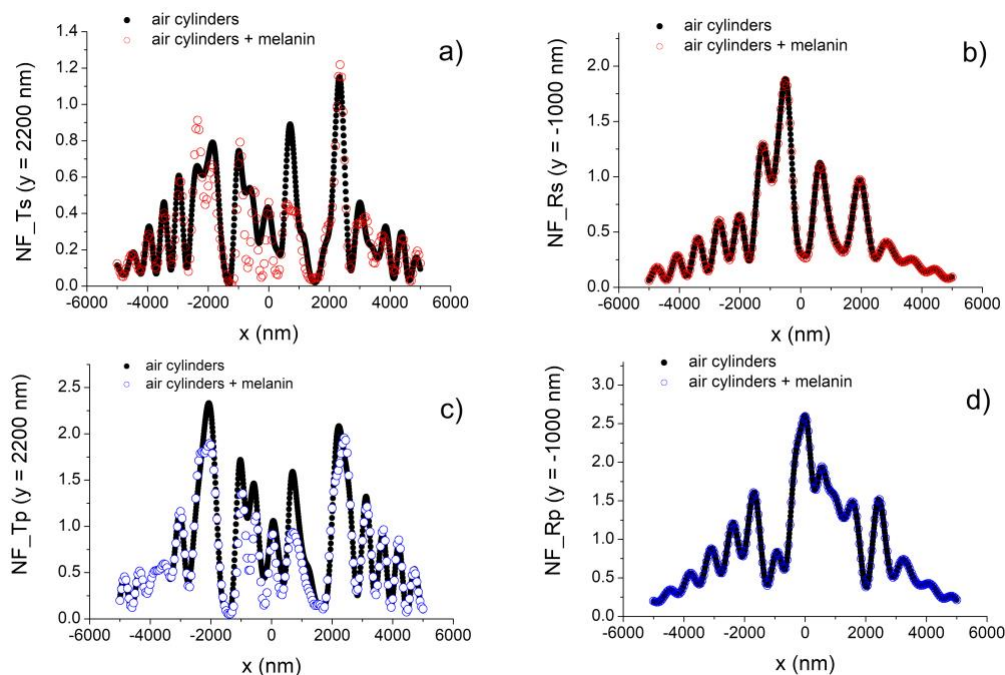


Fig. 5. Intensity distribution of the total near field (NF) at $\lambda = 650$ nm for the systems with and without basal melanin considered in Fig. 4, evaluated at two different y -levels: $y = 2200$ nm (transmitted field, (a) and (c)) and $y = -1000$ nm (incident and reflected field, (b) and (d)). Panels (a)-(b) correspond to S polarization and (c)-(d) to P polarization.

In order to investigate if the negligible effect of basal melanin is a general trend, in Fig. 6 we show the reflectance curves for another system comprising cylinders of the same size as in Fig. 4, but distributed in a different way. In this case, the positions of the melanin cylinders were chosen so as to partly surround the air ones (see Fig. 6(c)). Although there are slight differences between the reflectance of the system with and without basal melanin for short wavelengths for both polarization modes, they are not significant.

To find a relationship between the reflected response of the regular and the weakly disordered structures, a fast Fourier transform of the cross-section images of both systems were performed, and the results are shown in Fig. 7. Basically, the Fourier transform reveals three characteristics of the analyzed structure: the shape and extent of the whole system, the shape and size of the individual elements, and the nature of the arrangement. For the hexagonal arrangement (Fig. 7(a)), the Fourier transform exhibits a pattern of regularly distributed high intensity peaks, which reveals the perfect periodicity, modulated by the diffraction pattern of an individual circle, i.e, a central disk surrounded by concentric rings. As expected, these rings are also found in the Fourier spectrum for the disordered system (Fig. 7(b)),

indicating that the scattering objects are of equal size and shape. The radius of the central circle in the (k_x, k_y) -space (highlighted in yellow), is approximately $2\pi/r$, r being the circles' radius. However, the Fourier transform of the weakly disordered system shows a uniform intensity distribution in the (k_x, k_y) -space, indicating that the system presents a certain degree of isotropic disorder. Similar Fourier spectra were obtained from the spongy structures found in the barbs of some birds' feathers [30].

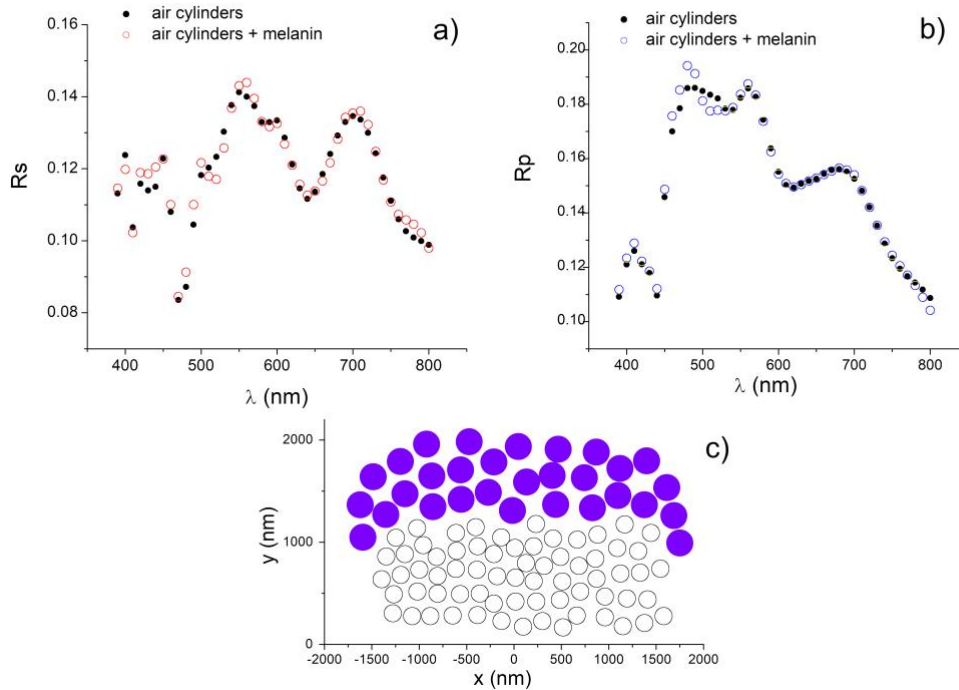


Fig. 6. Reflectance of another realization of a weakly disordered arrangement of cylinders immersed in keratin, with (hole circles) and without (solid black dots) basal melanin, for S (a) and P (b) polarization. (c) Scheme of the cross-section of the analyzed structure (the colored circles indicate melanin).

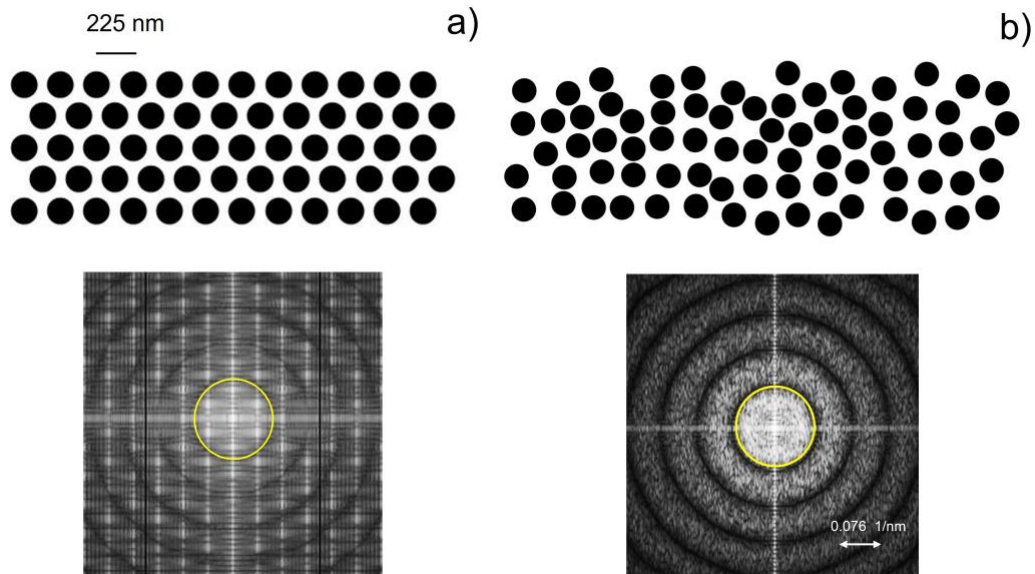


Fig. 7. (a) Hexagonal system of 5 layers of cylinders considered in Fig. 3 and its Fourier transform. (b) Weakly disordered arrangement of cylinders considered in Fig. 4 and its Fourier transform.

The optical response of this type of disordered structure can also be estimated by studying its structural correlation, together with the scattering mean free path l_s or the transport mean free path $l_t = l_s/(1 - g)$, with g being the scattering anisotropy factor ($|g| < 1$, $g > 0$ indicates forward scattering and $g < 0$ denotes backscattering). It describes the average distance required for light to become diffusive (for example, for constant l_s and forward scattering, l_t increases). For propagation distances much greater than l_t , a lightbeam becomes almost isotropic [31].

From this information, it can be determined if the propagation of electromagnetic waves in the medium is dispersive, highly dispersive (as the weakly disordered structure studied in this work), or diffusive. The transition from a dispersive to a diffusive medium is determined solely by l_t and the total thickness of the composite medium. For the example considered in Fig. 7(b), some characteristics of the periodic hexagonal structure (which serves as starting point of this arrangement) can be observed. The optical response of the system contains the information provided by the quasi-ordered clusters that comprise it, such as a pseudo-band gap [32, 33]. Ultimately, the total thickness of the dispersive medium will govern the optical response, as recently noticed in the feather barbs of the Eurasian jay [6].

3.b. Structures Formed by Spheres

To extend our study and investigate the effect of basal melanin in 3D structures, in this Section we consider a hexagonal matrix of air spheres with $R = 82.7$ nm, $a = 225$ nm and $M = 5$, as schematized in Fig. 2. In Fig. 8 we show the reflectance curves for the structure with and without two additional layers of melanin spheres of radius $R_m = 110$ nm also distributed in a hexagonal arrangement with the same lattice constant. The spectra shown correspond to both polarization modes, which coincide for normal incidence. As expected for a regular structure, an intensification of the reflectance is observed within the band gap spectral region, with a maximum of approximately 55% at $\lambda = 550$ nm. As in the case of the cylinders' structure (Fig. 3), it is observed that the basal melanin does not significantly affect the reflected response of the structure within the band gap; both curves slightly deviate from each other only outside the band gap. It is important to remark that similar results were obtained by adding more layers of melanin (not shown): the reflectance response remains almost unchanged and only slight changes are observed for wavelengths larger than those of the band gap.

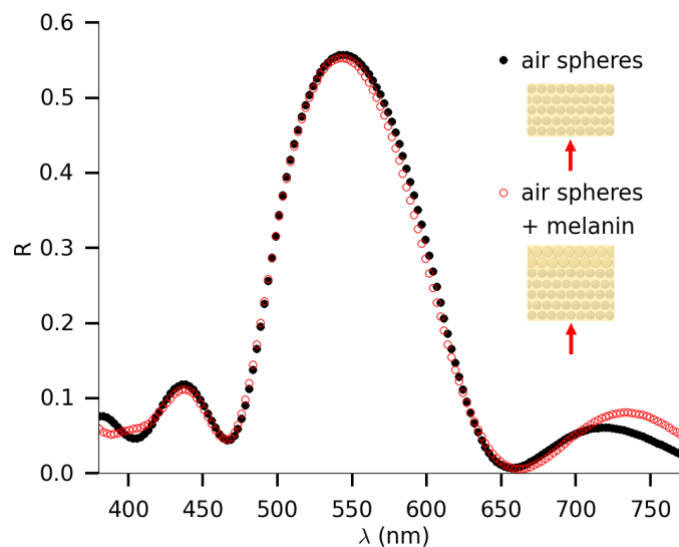


Fig. 8. Reflectance of a hexagonal matrix comprising 5 layers of air spheres immersed in keratin, with (hole circles) and without (black solid dots) two additional layers of melanin spheres. The insets schematize the structures considered.

4. Discussion and Conclusions

The effect of basal melanin in the optical response of perfectly regular and weakly disordered photonic crystals comprising air scatterers in a keratin matrix was investigated. Two extensively used rigorous

electromagnetic methods have been employed in order to embrace a larger variety of structures. To analyze 2D systems comprising infinite cylinders we used the integral method, whereas the KKR method was employed to deal with 3D spheres' photonic crystals.

The simulations presented show that, regardless of the characteristics of the air elements comprising the system, such as spherical or cylindrical inclusions, perfectly regular or weakly disordered distribution, the effect of melanin on the reflectance spectra is practically null for the studied structures, which comprise inclusions of typical sizes and separations as those found in the nanostructures of avian feather barbs. This result is in agreement with the results of Ref. [6] for the Eurasian jay plumage, in which the authors found that although the SM present in the feather barbs is backed by melanin granules, the variations in thickness of the SM is the only responsible for the color change.

The weak influence of basal melanin in the optical response holds for both, finite arrays of cylinders and infinite systems of spheres. This confirms that, in many cases, electromagnetic methods designed for infinite periodic structures, which are usually less computationally demanding, can adequately describe the optical properties of systems with a finite number of scattering elements.

It is worth mentioning that there are previous studies on the color of bird feathers that combine a spongy matrix and melanin granules in their barbs, in which melanin is given an essential role in color generation. This study is not intended to rule out this possibility. Avian feathers are very complex systems that comprise different materials, varied geometries, etc., features that were only partially accounted for by the proposed models. For example, the degree of disorder present in the spongy matrix could have a significant impact on the reflected response, and therefore, it would be interesting to consider a higher degree of disorder in the location as well as in the size of the scatterers. Another element that has not been taken into account in this study is the keratin cortex that surrounds the barb, its thickness, curvature and irregularities, which most likely affect the observed color. Therefore, more research is needed to give a more determinant conclusion.

Acknowledgments. G.U., M.I. and D. S. acknowledge financial support from Consejo Nacional de Investigaciones Científicas y Técnicas (PIP 11220170100633CO) and Universidad de Buenos Aires (UBACyT 20020190100108BA). G.U. acknowledges Universidad de Buenos Aires, Argentina, for a doctoral Scholarship. M.L acknowledges financial support from Agencia Nacional de Promoción de la Investigación, el Desarrollo Tecnológico y la Innovación (PICT-2018-04535) and Universidad Nacional del Centro de la Provincia de Buenos Aires.